Geostatistical filtering to map a 3D anthropogenic pedo-geochemical background for excavated soil reuse

Baptiste Sauvaget, Chantal de Fouquet, Cécile Le Guern, Didier Renard, Hélène Roussel

Version of Record: https://www.sciencedirect.com/science/article/pii/S0375674222000899
Manuscript_3f795a96906701e49e052a34198f38e9

Geostatistical filtering to map a 3D anthropogenic pedo-geochemical background for excavated soil reuse

Baptiste Sauvaget [a, b, c], *Chantal de Fouquet* [b]
Cécile Le Guern [a, d]*, *Didier Renard* [b], *Hélène Roussel* [c]

[a] *BRGM, Direction Régionale des Pays de la Loire, Nantes, France*
[b] *Mines Paris Tech, Centre de Géosciences, Fontainebleau, France*
[c] *ADEME, Angers, France*
[d] *IRSTV, Nantes, France*

**corresponding author at BRGM, Direction Régionale des Pays de la Loire, Nantes, France*
e-mail address : c.leguern@brgm.fr (C Le Guern)

Abstract

The safe reuse of excavated soils in urban areas requires the guarantee of geochemical compatibility between this scarce resource and the local pedo-geochemical background. Previous works have shown that the usual statistical tools (high order quantiles, upper whiskers) are not always adequate for separating anomalies from background contents, especially when there are many anomalies.

This paper presents an application of factorial co-kriging (geostatistical filtering) used to separate anomalies from the pedo-geochemical background, according to their different scales of spatial variability. The hypothesis is that the background corresponds to long distance variations, while the anomalies, which can be either positive or negative,- represent short distance variations.

The variable of interest is the lead content (Pb) in the subsoils of the "Ile de Nantes" urban area, where some areas were previously dedicated to industrial activities. The data were collected from different surveys, not specifically aimed at determining the pedo-geochemical background, but rather in a context of pollution diagnostics. The lengths of the samples were strongly variable. In a first step, only the samples having approximately the same length were retained for the estimation, which significantly reduced the amount of data. In a second step, the geostatistical estimation was performed using all the data. The resulting maps are significantly more accurate for the total Pb and its background component. The distinction between anomalies and background is discussed based on the calculated maps.

Factorial co-kriging appears to be relevant to map the anthropogenic pedo-geochemical background, using data acquired for other purposes. It allows separating anomalies and background for any parameter presenting significant contrasts.

Keywords: separation, background, anomalies, geostatistics, filtering**,** geochemical

1 Introduction

Soils are located at the interface between the hydrosphere, the biosphere and the atmosphere, and are thus exposed to influences from various phenomena. Referring to Standard ISO 11074, the term "soils" will be used hereafter as it encompasses both soils and subsoils, including anthropogenic deposits. Soils can be heterogeneous and are known to show even greater heterogeneity in urbanized areas due to important anthropogenic impacts (Cicchella et al., 2008; Le Guern et al., 2016a, 2016b ; Madrid et al., 2006; Pouyat et al., 2007; Rodrigues et al., 2009). Heterogeneity may cause major difficulties when identifying general properties of the environment

or building reference databases (Ander, 2013; Demetriades and Birke, 2015). This is why the data acquisition step is typically focused on a specific phenomenon, e.g. the measurement of metal content (Ander, 2013; de Fouquet, 2011; Lark and Scheib, 2013; Saby *et al.*, 2006), the evaluation of carbon stock (Edmondson *et al.*, 2012; Raciti *et al.*, 2012) or the determination of biological indicators (Hartley *et al.*, 2008). Faced with the problem of soil heterogeneity, previous authors; e.g., Demetriades and Birke (2015) for urban topsoils, have proposed sampling strategies focused on the "most representative sampling sites" for determining threshold values to define the urban pedo-geochemical background. However, anomalies may often still be present in the final data. Such anomalies are related either to the specificities of the particular medium (local contamination, different soil composition or rearrangement) or to analytical errors: therefore they are not representative of the studied environment and phenomena. The presence of anomalies is even more pronounced when using preexisting data, since the sampling strategies were not defined for the specific objective of the study at hand. This is the case for instance in France for redevelopment projects. In France, in the absence of generic soil quality thresholds at a national level, the reuse of excavated soils must refer to local soil background values. However, the geochemical data available to determine this local background mainly come from pollution diagnostic studies." Therefore such data contain many "outliers" also referred to as "anomalies". The objective of this paper is to propose a coherent methodology for addressing such anomalies in the context of pedo-geochemical background determination.

A manual data sorting, performed by an expert with detailed knowledge of the issues and settings, may be efficient although time-consuming and results may vary from one operator to another. Semi-automatic sorting methods are thus preferred in order to separate the background (i.e. the studied feature) from the anomalies. Threshold values used to separate anomalies within a set of representative data are usually calculated using statistical criteria. Such thresholds are often based on higher-order quantiles (Q90 or Q95; Ander, 2013; Cave *et al.*, 2012; McIlwaine *et al.*, 2014; Rothwell and Cooke, 2015) or on the sum of two terms; i.e., a "central" term (mean or median) and a dispersion-dependent term. Common examples are the upper whisker (Jarva *et al.*, 2014; Leys *et al.*, 2013; Reimann *et al.*, 2005, 2018; Reimann and de Caritat, 2017; Rothwell and Cooke, 2015; Tarvainen and Jarva, 2011) and the MAD (Median Absolute Deviation) thresholds (Leys, 2013; Reimann *et al.*, 2018). However, "outliers" isolated in this manner only include "extreme" values (which are usually the largest). Among other factors, the results are influenced by the distribution, the sample size, the censoring rate and the actual anomaly rate of the data (Reimann *et al.*, 2005; Rothwell and Cooke, 2015; Sauvaget, 2019; Sauvaget *et al.*, 2020). These statistical criteria may ultimately prove to be inappropriate in determining anomalous data in the case of data collected in a different context with different objectives (Sauvaget *et al.*, 2020).

The classical framework for estimating statistical thresholds consider data as randomly and independently drawn Butdata can also be interpreted as realizations of a sampling process applied to a regionalized variable displaying some inherent spatial variability. This spatial variability is described and quantified by the variogram, which expresses the relationship (up to the factor 1/2) between the mean quadratic deviation of the data and their spatial distance. This variogram is then used to estimate the variable at unknown locations by co-kriging. Even though geostatistics was initially developed for mining applications (Matheron, 1965), the factorial kriging or co-kriging designed for the search of local anomalies has a wide range of applications in soil sciences (Matheron, 1982; Goovaerts, 1992; Wackernagel and Sanguinetti, 1993 ; Bourennane *et al.*, 2003 ; Rivoirard, 2003; Saby *et al.*, 2009). The approach relies on the different scales of spatial variability present in the data. A variable component associated to each given scale can then be estimated by factorial kriging or co-kriging.

The pedo-geochemical background (Ademe Agency, 2018; Baize, 2008; Daniau *et al.*, 2009; Reimann *et al.*, 2005) reflects the full set of usual soil contents throughout the study area. It

represents either natural phenomena or diffuse contamination and differs from localized contamination or natural anomalies. Given that systematic sampling campaigns for determining pedo-geochemical background values in urban areas are not currently pursued in France, the use of preexisting non-specific data (primarily stemming from pollution diagnostic studies characterizing soils and subsoils) is necessary. This constraint introduces a lack of representativeness in the data, which can be expected to contain a larger proportion of anomalies due to the initial sampling objectives. This introduces additional difficulties for the determination of a local pedo-geochemical background, as it requires a careful separation of anomalies. The development of appropriate methods is therefore needed. In the context of the reuse of excavated (sub)soils in France, an additional difficulty lies in the 3D approach needed to determine the volumetric pedo-geochemical backgrounds that will be used as reference values (Coussy *et al.*, 2020).

In this paper, the relevance of factorial co-kriging (geostatistical filtering) for estimating pedo-geochemical background values is examined in the context of local volumetric analysis for guiding the reuse of excavated (sub)soils. The underlying hypothesis is that the "background" corresponds to long-distance variations (i.e. long range), while the "anomalies" correspond to short-distance variations (short range) with respect to the working scale.

2 Presentation of the site and collected data

The data were collected within an urban district located in central Nantes (France). This district is composed of former islands on the Loire River, backfilled during the 20th century to form a single island in the middle of the river, measuring 4.9 km long by 1 km large and covering a land area of 337 hectares. District population is approx. 18,000, representing on the order of 6% of total city population. The geological context is mainly composed of a thick layer of anthropogenic deposits, with a thickness varying between 2 and 5 m. These deposits are classified according to the intrinsic contamination potential of the backfill material (Le Guern *et al.*, 2016 a, b): i) man-made grounds with a high intrinsic contamination potential, ii) various man-made grounds with a medium intrinsic contamination potential iii) natural sandy deposits (corresponding to sediments dredged from the Loire River) showing a low intrinsic contamination potential. Below this layer, Loire River alluvia (up to a thickness of 20 m) are lying on micaschists (Le Guern *et al.*, 2016a, 2016b).

The previous industrial activity on the site is related primarily to the port and shipbuilding yards located in the western part of the island. This activity gradually declined until the closure of the last yards around 1987. It was followed by a district revitalization plan (2000-2030). The volume of excavated soils linked to renovations in the district's southwest sector has been estimated at roughly 100,000 tons per year from 2015 to 2025. In order to reuse the excavated soils, the land developers need to refer to the local volumetric pedo-geochemical background, with respect to individual trace element and persistent organic substance contents of the soils and subsoils. In the absence of a information at this scale based on existing national sampling campaigns, the local office of the French Geological Survey (BRGM) used readily available data from existing soil studies (Le Guern *et al.*, 2016a, 2016b, 2017a). The data are from 2,570 boreholes and 2,120 samples, mostly in relation with soil contamination diagnostics. The boreholes are georeferenced in a database built using Microsoft Access 2010 which also provides the descriptions of the various layers identified, the top and bottom depths of the collected samples and the analytical sampling results. Figure 1 shows the distribution of these data with an indication of the type of study. The geochemical data come from the pollution diagnostic studies.

In a first approach, the data processing was simplified by considering a vertical succession of 2D-layers, corresponding to various types of anthopogenic deposits and alluvia, with different properties. Most samples refer to one layer, within the first five meters of depth. This depth

corresponds to the maximum depth for future buildings, and therefore of excavation or reuse of soil materials. The compositions of the samples serve to assign them to the different types of deposits. A sample crossing several types of materials (at the interface between two layers) is not taken into account in the analysis since the objective is to define a pedo-geochemical background per individual layer.

We first focus on the natural-like made-grounds composed of sandy Loire River dredged sediments, which are present within the entire district. 589 samples are associated with this type of made-ground, among which 581 show copper, lead and zinc contents analysed by ICP-MS following extraction with *aqua regia*. These three metals are indicative of anthropogenic impacts (Alloway, 1990; Birke and Rauch, 1997, 2000) within this district. Because their contents present a high level of linear correlation (Table 1), only the results for lead will be presented in this paper.

Table 2 gives the statistical summary of the Pb contents. For reference, the statistical thresholds of the pedo-geochemical background obtained for lead on the processed data (all the 581 samples) are given in Table 3. The MAD is lower than the other statistical thresholds, and just over the median (10 mg/kg_DM).

It is important to note that the length of the samples is highly variable, because they have been collected by different operators (see §3.2.1). This variation of the "support" has an influence on metal content variability (variance, variograms) and hence on the statistical and geostatistical processing. It was therefore necessary to take this data variability into account and a reduced dataset was considered where all samples have similar length (303 samples). We will refer to the whole dataset (581 samples) when using the complete dataset where all samples have different lengths.

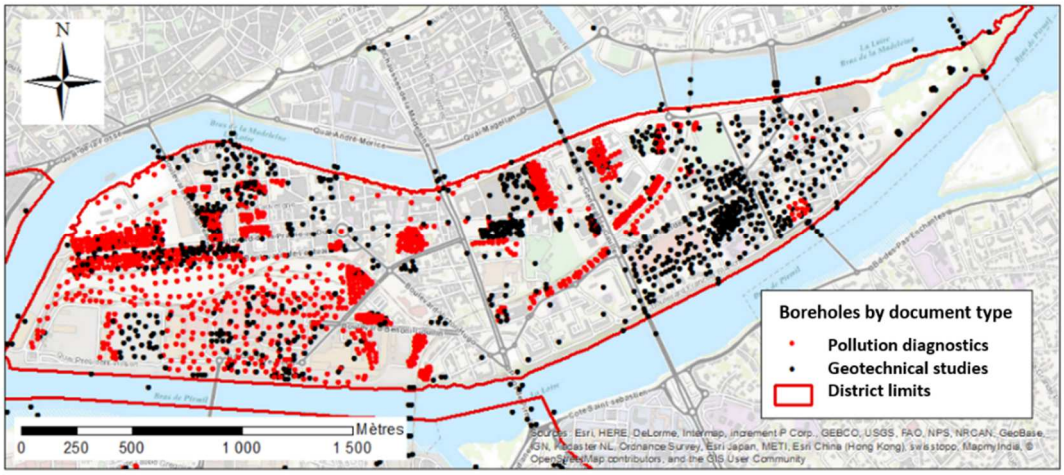

Figure 1: Map of the borehole data locations, with an indication of the type of study

Table 1: Correlation matrix of the copper, lead and zinc analyses on the hydraulic sandy made-grounds sampled within the Ile de Nantes district. Results in bold are based on the 581 samples of the whole dataset (whole dataset), while those in italic are based on the303 samples with similar sample lengths (reduced dataset).

CORRELATION MATRIX			
	Cu	**Pb**	**Zn**
Cu	1	*0.85*	*0.89*
Pb	**0.86**	1	*0.84*
Zn	**0.88**	**0.83**	1

Table 2: Statistics of Pb contents on the hydraulic sandy made-grounds within the Ile de Nantes district. Whole

dataset (581 data) and reduced dataset (303 data). Units are mg/kg of dry matter.

Pb	Min	Max	Median	Mean	StDev	CV
Whole dataset (581)	3.0	240	10	20.4	27.6	1.35
Reduced dataset (303)	5.6	240	13	27.5	35 .0	1.27

Table 3: Pedo-geochemical background threshold values of Pb contents calculated by different statistical methods on the hydraulic sandy made-grounds over the Ile de Nantes district. Units are mg/kg of dry matter.

Pb	Upper whisker	MAD	Q90	Q95
Whole dataset (581)	28.4	15.4	32.5	40.3
Reduced dataset (303)	57.5	21.9	56.9	92.3

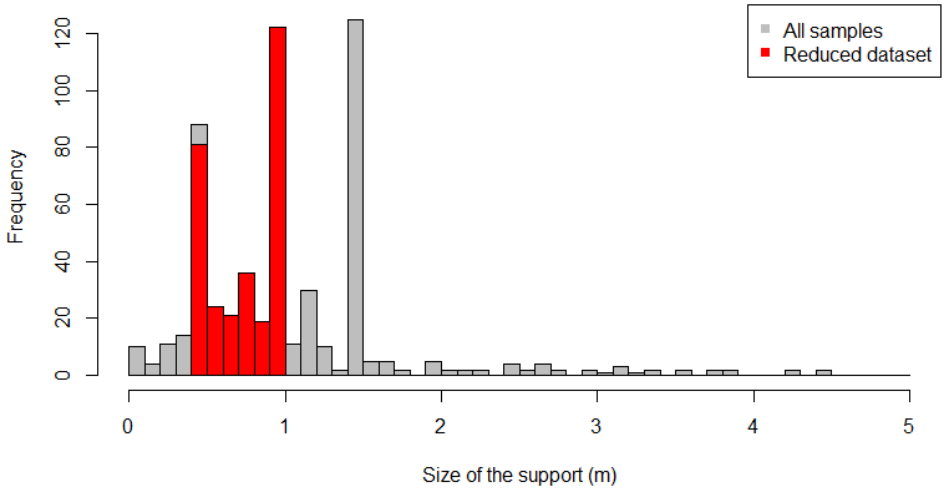

Figure 2: Thickness of the 581 samples (whode dataset). In red, the 303 samples of the reduced dataset.

3 Methodology

3.1 Geostatistical filtering by factorial co-kriging

The aim of the proposed methodology is to separate the anomalies from the background as illustrated schematically in Figure 3. Factorial co-kriging provides a geostatistical technique to filter the anomalies characterized by short-distance variations, from the geochemical background associated with long-distance variations.

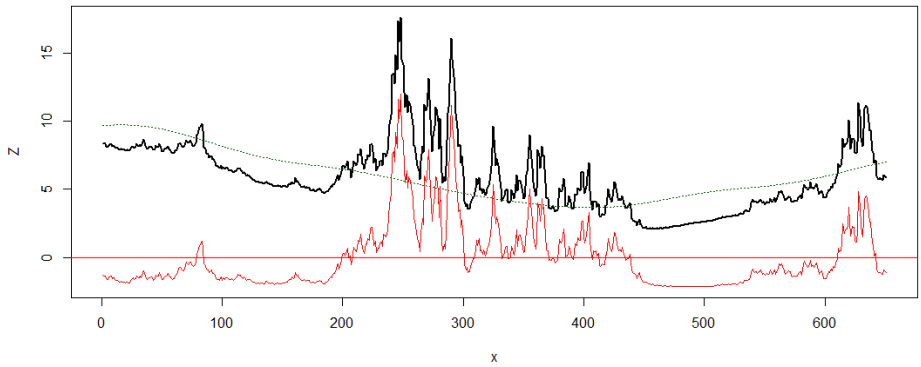

Figure 3: Decomposition of total content $Z(x)$ (bold black line) as the sum of short-distance $Y^1(x)$ (red thin line) and long-distance $Z^2(x)$ variations (green dots). Long-distance variations are interpreted as the geochemical background. The spatial mean of anomalies equals zero. The distance unit in abscissa is arbitrary.

Factorial co-kriging relies on an interpretation of the variogram model with several structures (in the monovariate case) and of the linear model of coregionalization (in the multivariate case). The monovariate case is first discussed, and the multivariate case is presented later. Hereafter, co-kriging will refer to the usual co-kriging of the total content, and filtering to factorial co-kriging of the long-range component.

3.1.1 Monovariate case

The Pb content is modeled as a random function $Z(x)$ which is assumed to be stationary of order two (for the sake of simplicity): i.e. its expectation (probabilistic mean) m is constant and the spatial covariance between $Z(x)$ and $Z(x+\vec{h})$ only depends on $\vec{h}$ (simply denoted h in the following). The variogram $\gamma(h)$ is assumed to be the sum of two structures γ^1 and γ^2 (where 1 and 2 refer to indices in all the subsequent equations):

$$(1)\quad \gamma(h) = \gamma^1(h) + \gamma^2(h)$$

The random functions $Z(x)$ may be written as the sum of a constant expectation m, and a linear combination of two spatially uncorrelated components $Y^1(x)$ and $Y^2(x)$ with a zero expectation (yielding a zero cross variogram):

$$(2)\quad Z(x) = Y^1(x) + Y^2(x) + m$$

In this decomposition the variogram of Y^1 is γ^1 and that of Y^2 is γ^2.

When the ranges of the two components are significantly different, it is reasonable to regroup the expectation with the longest-range $Y^2(x)$ component (Rivoirard, 2003):

$$(3)\quad Z(x) = Y^1(x) + Z^2(x)$$

where $Z^2(x) = Y^2(x) + m$.

Each component may be estimated by co-kriging from the Z data (Wackernagel and Sanguinetti, 1993). In classical terms, the co-kriging matrix involves the variogram γ between Z data, whereas the right-hand side of the system considers the cross variogram between Z data and the variable to be estimated, i.e. $\gamma^1(h)$ for the "anomalies" Y^1 and $\gamma^2(h)$ for the "long-range" component Z^2 associated with the pedo-geochemical background.

To estimate the long-range component Z^2 (with the same expectation as Z), the non-bias condition imposes that the sum of the factorial co-kriging weights equals 1. Conversely, the expectation of $Y^1(x)$ being zero, then the non-bias condition for estimating anomalies imposes that the factorial co-kriging weights add up to zero.

These results can be generalized to the intrinsic case; for example when the variogram of the "background" presents a linear structure (i.e. unbounded variogram). In this case, the non-bias conditions become authorization conditions (Chilès and Delfiner, 1999).

3.1.2 Multivariate case

The following discussion relies on the properties of the linear model of coregionalization (Bourennane *et al.*, 2003; Goovaerts, 1992; Rivoirard, 2003; Saby *et al.*, 2009; Wackernagel and Sanguinetti, 1993). As for the monovariate case, the presentation is made in the case of stationarity of order two.

According to this model, the simple and cross variograms of all variables are linear combinations of the same basic structures (Chilès and Delfiner, 1999). For the pair of variables denoted i and *j,* all simple and cross variograms are written as follows:

$$\gamma_{ij}(h) = \sum_k b_{ij}^k \ \gamma^k(h) \quad (4)$$

where γ^k stands for the normalized variogram with rank k (sill equal to 1).

The set of simple and cross-variograms can be written in a synthetic way using a matrix form, i.e.:

$$[\gamma_{ij}(h)] = \sum_k [b_{ij}^k] \ \gamma^k(h) \quad (5)$$

where the sill matrices $\left[b_{ij}^k\right]$ must be symmetrical and of a positive type. Therefore, a structure is present in a cross-variogram only if it is present in the two related simple variograms. Conversely, a structure can be present on simple variograms without necessarily appearing in the cross-variograms.

In this model, the variables themselves are decomposed into linear combinations of spatial independent components corresponding to the full range of variability scales:

$$Z_i(x) = m_i + \sum_k {Y_i}^k(x) \quad (6)$$

where the expectations of the spatial components ${Y_i}^k$ are null.

Like in the monovariate case, the "mean" m_i is regrouped with the long-range component of each variable. Thus we wish to estimate the values linked to the longest-range component(s), in order to filter out short-range variability.

3.1.3 Use of "explanatory" covariates

To specify the choice of the component(s) to be assigned to the "background" or to "anomalies", some attention should be drawn to the correlation matrix deduced from the variance-covariance matrices that can be calculated either globally or by structure using the relevant formula:

$$r_{ij} = \frac{Cov\,(Z_i,Z_j)}{\sqrt{Var\,(Z_i)}\,\sqrt{Var\,(Z_j)}} \text{ and } r_{ij}^k = \frac{b_{ij}^k}{\sqrt{b_{ii}^k}\sqrt{b_{jj}^k}} \quad (7)$$

where r_{ij} is the linear correlation coefficient between variables i and *j*, and r_{ij}^k the regionalized coefficient associated with component *k*, with $Cov\left(Z_i,Z_j\right)$ representing the covariance between variables i and *j*, and $Var(Z_i)$ and $Var\left(Z_j\right)$ their respective variances.

The correlation matrix per spatial structure reflects the various links between variables, with respect to the spatial variability scale. This result is of special interest herein because it enables

drawing the link between the targeted contents and the covariates. This in turn can be used to select the component(s) retained to estimate the pedo-geochemical background: for example, correlated components present for different metal associated with the same anthropic contamination (eg. Pb, Zn, Cu).

According to the formula (6), by solely selecting the longest-range component ${Z_1}^2$ for the content Z_1 background estimation, we can express:

$$Z_{1,BG}(x) = {Y_1}^2(x) + m \quad (8)$$

This component is estimated by factorial co-kriging based on the Z_1 data (eg. Pb) with one covariate Z_2 (eg. Cu or Zn) or several covariates $Z_{i>1}$(eg. Zn and Cu) potentially known more densely (eg. land use) and whose "long-range" component is adequately correlated with that of the Z_1contents.

3.2 Taking into account sample lengths

As mentioned in section 2, the data used here correspond mainly to pollution diagnostic studies. They were collected by different operators and were not originally acquired for the determination of an anthropized pedo-geochemical background. Therefore, the lengths of the samples do not correspond to the heights of the soil formations. We therefore do not have sufficient information to use an accumulation model. As a consequence, in order to take into account the variable lengths of the samples, two approaches are compared. The first one is a selection of the data with a length close to the mode of the length histogram. The second approach consists in introducing explicitly the sample support in the co-kriging (and filtering) calculations, using data discretization (Lark & Scheib, 2013; de Fouquet, 2019).

3.2.1 Selection of data based on length

In this approach, only the samples with an almost similar length are retained. The sample lengths of the whole dataset lie between 0.1 and 4.5m with three modes on the histogram: 0.5m, 1m and 1.5m (Figure 4). To keep most of the samples while preserving the spatial distribution of the data and a relatively constant sample length, we consider samples with support between 0.5m and 1m inclusive. This selection reduces the number of samples from 581 (whole dataset) to 303 (reduced dataset). This selection discards a large proportion of low contents and influences the general statistics of the Pb contents as can be seen in Table 2: the median, the mean and the standard deviation increase, whereas the coefficient of variation slightly decreases. However, the correlation coefficients of Pb with Cu or Zn remain similar.

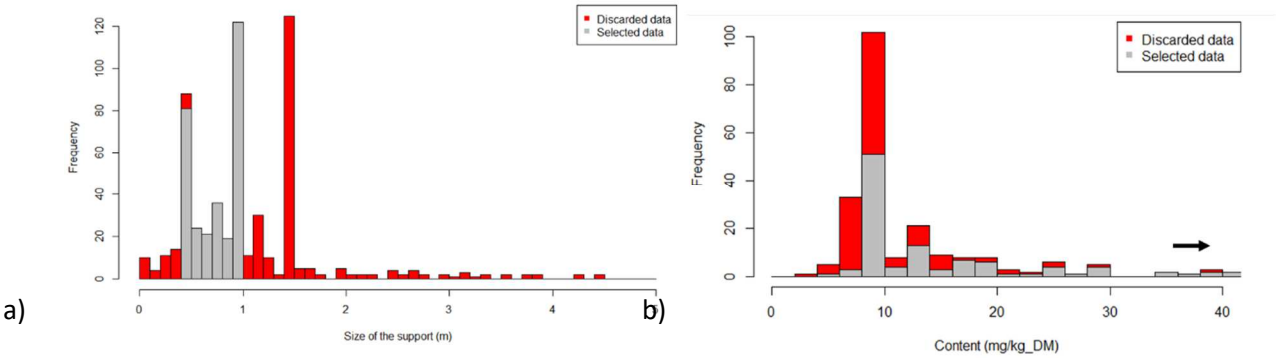

Figure 4: Histogram of sample length (a) and of Pb contents (b) for the complete (581 data) and the reduced (303 data in grey) datasets.

The statistical thresholds of the pedo-geochemical background for Pb, calculated on the selected 303 samples, are much higher than for the initial sample set (Table 3), especially for the Upper whisker and the Q95 (57.5 vs 28.4 mg/kg_DM, 92.3 vs 40.3 mg/kg_DM respectively). This shows the important sensitivity of those criteria to the sample population. This variation reflects the fact that discarded data mainly correspond to lower Pb values as shown in Figure 4 and 5.

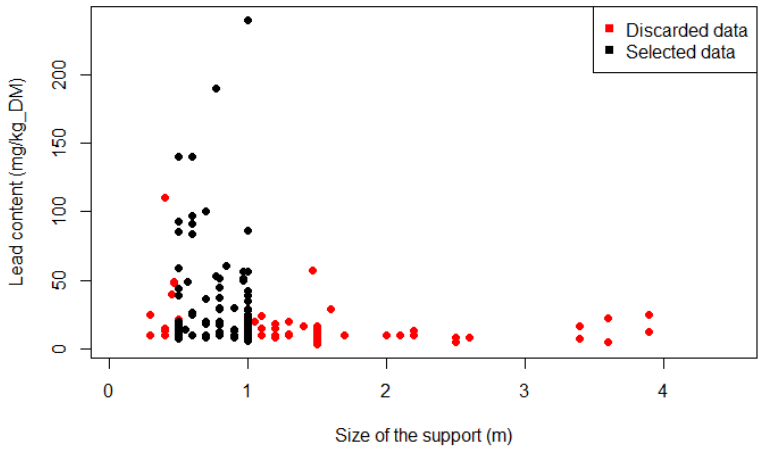

Figure 5: Scatter plot between sample length and Pb contents for the complete (581 data) and the reduced dataset according to length (303 data in black).

3.2.2 Co-kriging with a multi-support dataset

The aim is to enable the use of all 581 samples for the estimation by co-kriging and filtering despite their different support. However, the variographic analysis is performed with data having roughly the same support, i.e., the reduced dataset with sample lengths between 0.50 m and 1 m. For the calculations explained hereafter, this length L is supposed to be equal to 0.75 m. As only one sample per borehole generally belongs to the target layer, only the horizontal sample variogram is calculated, but this sample variogram will be assumed to be isotropic for 3D calculations. To take into account the various sample lengths in the estimation step, the samples are discretized into segments of smaller length d (here d=0.1 m). The d support variogram is deduced from the L support model of variogram. The d support variogram is supposed to be horizontally isotropic. The nugget effect is increased by the factor L/d. The vertical ranges are reduced by the distance d ; the horizontal ranges are not modified, as cores are vertical. This modeling approach involves a slight approximation because it does not take perfectly account for the modification of the variogram shape at the origin.

The modeled d-support variogram is then used for the estimation. The sample length is taken into account in the matrix and in the right-hand side of the co-kriging system thanks to the length sample discretization into d-length segments.

3.3 Variographic analysis of the Île de Nantes data

The simple and cross horizontal variograms for Cu, Pb and Zn, are calculated for the district (15 calculation steps span 90m each, Figure 6). The fitted model comprises a nugget effect and two spherical structures with ranges of 200m and 1000m.

To determine long-range structures associated with the “background”, the regionalized correlation coefficients are examined (Table 4). The nugget component presents a strong correlation among the three metals. As stated before, the point-source contaminations are expected to be

similar for Cu, Pb and Zn. This nugget component reflects short-distance variations (vs horizontal distance between samples of about 90m) or other causes of heterogeneity.

The intermediate spherical component (200m range) shows correlation coefficients smaller than those of other components and those of the metals. Then the variations taken into account by this component differ between the three metals. We have chosen to filter this component out so as to only retain the highly-correlated variations for the pedo-geochemical background.

Lastly, the 1000m range spherical component exhibits a correlation between Cu, Pb and Zn larger than for the 200m range spherical component. The lower correlation between Pb and Zn, is mainly explained by the presence of a few samples with large Zn values and lower Pb contents. The long-range correlation among the three metals remains strong overall (Pb-Cu 0.89, Pb-Zn 0.77, Cu-Zn 0.98), compared to the coefficient correlations between total contents (Pb-Cu 0.85, Pb-Zn 0.89, Cu-Zn 0.89) (Table 1).

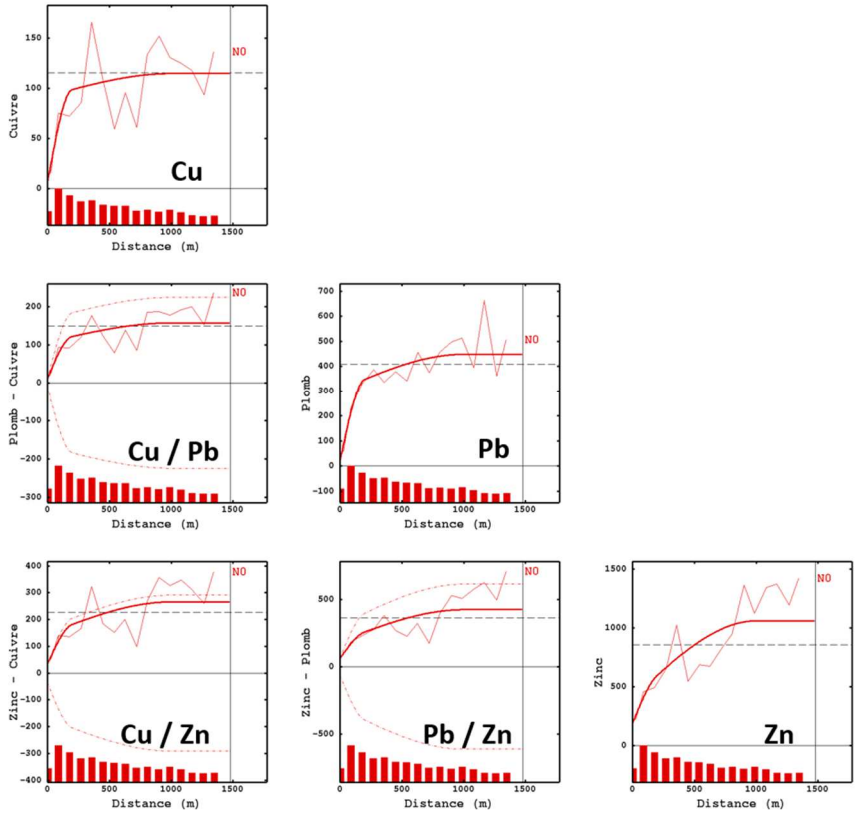

Figure 6: Simple and cross sample variograms of the Cu, Pb and Zn contents based on the reduced dataset (303 samples). The fitted model is shown as a solid red line. The histogram of the pairs is indicated. The grey dashed horizontal line indicates the variance in simple variograms and the covariance in cross variograms. The maximum correlation envelope (spatial correlation coefficient respectively equal to +1 or -1 for all structures) is indicated with a dashed red line.

Table 4: Regionalized correlation coefficients of Cu, Pb and Zn from the linear coregionalization model based on the reduced data set (303 samples)

	NUGGET EFFECT				**SPHERICAL: 200M**				**SPHERICAL: 1000M**		
	Cu	**Pb**	**Zn**		**Cu**	**Pb**	**Zn**		**Cu**	**Pb**	**Zn**
Cu	1.00			**Cu**	1.00			**Cu**	1.00		
Pb	**1.00**	1.00		**Pb**	**0.61**	1.00		**Pb**	**0.89**	1.00	
Zn	**1.00**	**1.00**	1.00	**Zn**	**0.83**	**0.51**	1.00	**Zn**	**0.98**	**0.77**	1.00

3.4 Tools and estimation domain

All calculations were carried out using the Isatis© geostatistical software and RGeostats. To perform the estimation, a modified version of the RGeostats co-kriging function was developed by MINES Paris Tech.

The estimations are performed at block support, on a grid covering the whole study area. The grid mesh is 10m by 10m by 0.75m. The estimations carried out with the reduced dataset (303 data, length between 0.5 to 1m) rely on a 2D approach: all the sample centers are assigned to the same horizontal depth at the center of the unique vertical mesh. The estimations carried out with the whole dataset (581 data) are based on a 3D approach, considering the exact vertical locations of the (discretized) samples.

4 Results and discussion

Table 5 presents the statistics of the block estimations of the total Pb and of the long-range components, for the whole and reduced datasets. It will help to discuss the estimation of the total Pb contents (co-kriging) and the Pb "background" component (filtering), based on the multivariate approach (using contents of Pb, Cu and Zn). The negative values are related to the negative weights of the kriging system. Post-processing would be necessary for these values. As this point is not specific to the methods of estimation used, it will not be discussed here. A possible correction would be to substitute these values by 0 or the limit of quantification (LQ) of the estimated parameter.

Tableau 5 : Statistics of Pb total content (co-kriging) and long-range components (filtering) according to dataset

	Estimated total content		**Estimated long range component**	
	whole dataset	***reduced dataset***	***whole dataset***	***reduced dataset***
Min	10.66	-5.26	-5.61	7.18
Max	124.84	173.02	58.27	70.03
Median	12.34	18.62	5.56	7.89
Mean	11.93	18.39	4.91	7.18
Standard deviation	12.33	17.37	6.58	5.25

4.1 Comparison of Pb background with total content estimations based on the reduced dataset

The maps of total Pb contents estimated by co-kriging and of the estimated Pb background values estimated by filtering using the reduced dataset (303 data), are presented in Figure 7. The estimated Pb contents (Figure 7) show highly contrasted areas (red and light blue spots). These spots indicate point-source contamination within the zone, as well as sites with abnormally low Pb contents compared to global statistics over the whole district. This is consistent with the extensive industrial past within the district's western sector and the presence of gasoline stations in the central-eastern part, as described in Le Guern *et al.* (2016a, 2017b). These spots with high or low contents are much smoother in the background estimation, which exhibits more homogeneity. The most homogeneous zones correspond to historical housings or former meadows now transformed into housings.

The higher-content areas seen in the estimated background in the western portion of the district can be explained by the presence of an industrial zone that has caused Pb contamination (Le

Guern *et al.,* (2016a, 2017b). This contamination, which affects a broad zone, is interpreted as diffuse contamination at the scale of the district.

The background estimation is less dispersed than the total Pb estimation (Figure 8). More specifically, since the estimated pedo-geochemical background only includes long range variations, the local contrasts are reduced out. The maximum estimated total content level is greater than that of the estimated background, which is consistent with the filtering of positive anthropic anomalies.

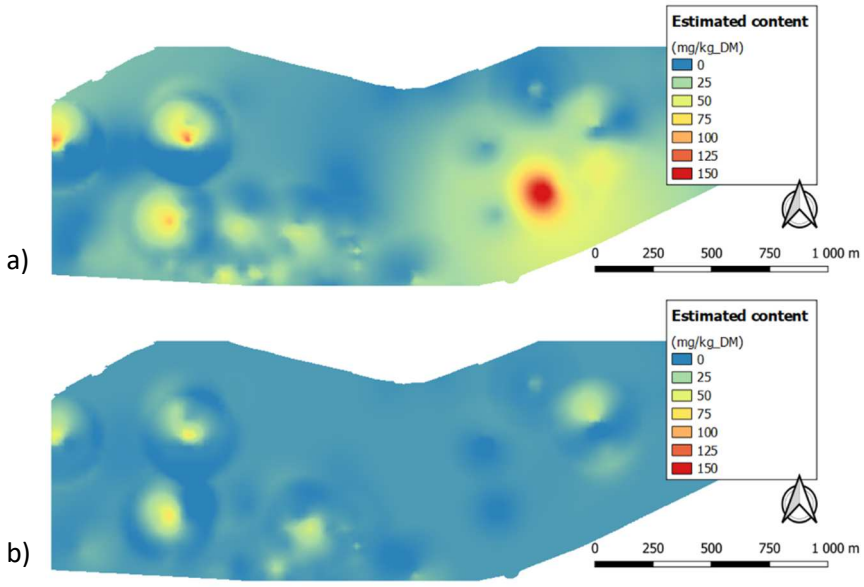

Figure 7: Block estimation of Pb contents by co-kriging (a) and pedo-geochemical background by filtering (b) based on the reduced dataset (303 data).

In Figure 8, the reported standard statistical thresholds (Q90, Q95, upper whisker and MAD threshold) are those calculated based on the whole dataset (581 data) in order to facilitate the further comparison with Figure 10 (cf. section 4.3). The MAD threshold (15 mg/kg_DM) is slightly lower than the mode of the background estimation (15 mg/kg_DM), whereas the upper whisker and the 90th quantile correspond to the high background estimated values. The 95th quantile is slightly lower than the maximum of the estimated long-range component.

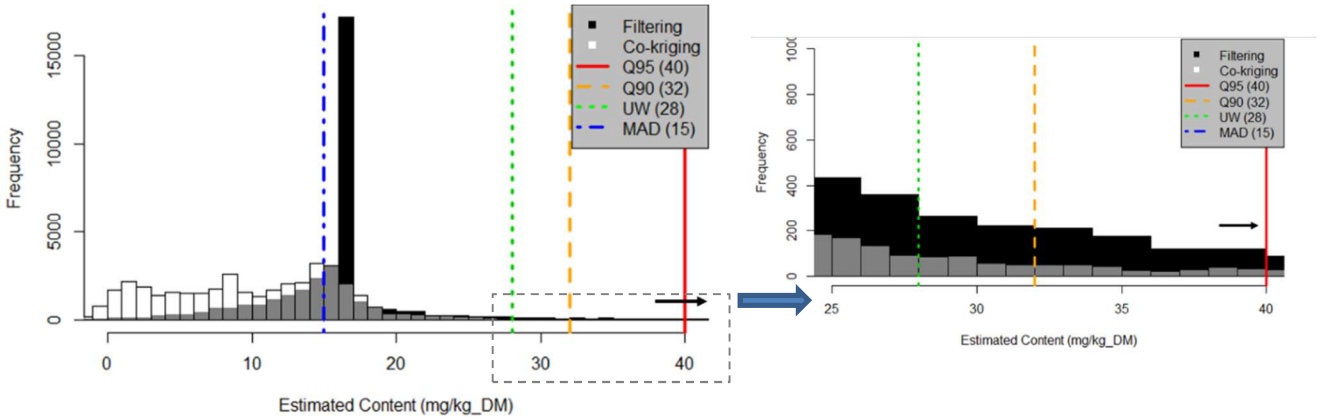

Figure 8: Histograms of estimated total Pb contents (grey and white) and estimated background (grey and black) based on the reduced dataset (303 data). The black arrow indicates graphic truncation (largest content around 140 is not shown). Standard statistical thresholds values calculated on the whole dataset (581 data) are reported. MAD: median absolute deviation, UW: upper whisker, Q90: 90th percentile, Q95: 95th percentile. Units are mg/kg_DM.

4.2 Comparison of Pb background with total contents estimations based on the whole dataset

The maps of the total Pb contents and of the Pb background estimated using the whole dataset (581 data) are presented in Figure 9. As in the case of the reduced dataset (Figure 7), the map of estimated total Pb contents shows highly contrasted values (red and light blue spots). Local contaminations are indicated by orange and red spots. Again the estimated background is more homogeneous than the estimated total contents.

However, some "polarized" background estimations (rapid changes from low to high values) appear in the area marked with the black circle in Figure 9. This is explained by the presence of a sample with large Pb content close to one with a lower content. This was not apparent when the reduced dataset was used because the sample with the largest value was discarded.

The histogram (Figure 10) confirms the lower dispersion of the estimated background compared to the estimated total contents. The total estimated contents show secondary modes around 15 and 22 mg/kg_DM. The mode of the estimated background values lies around 11 mg/kg_DM. The MAD threshold (15 mg/kg_DM) is higher than the main mode of the background component, and lower than the secondary modes of the estimated total Pb. The upper whisker and the 90th percentile are higher than the estimated background and the secondary modes of the estimated total Pb.

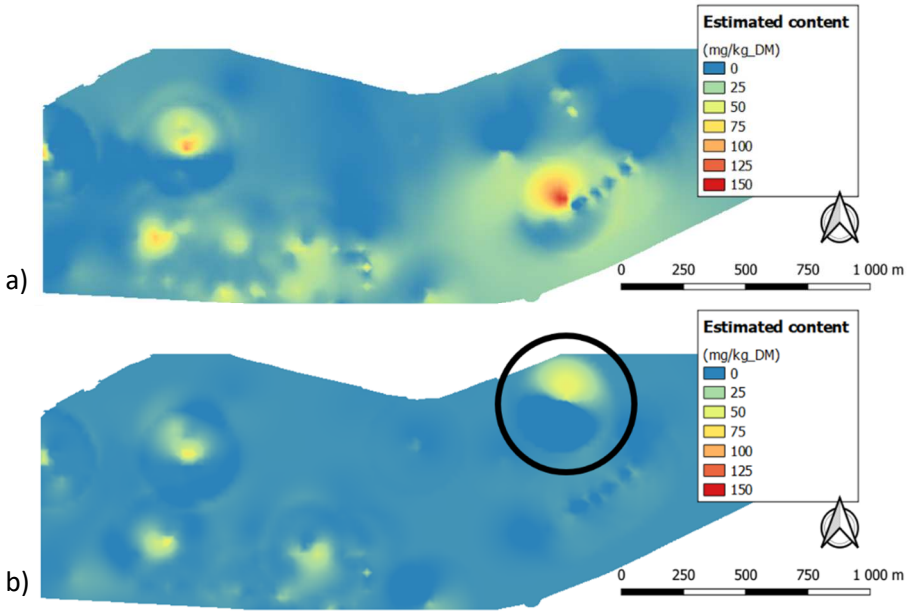

Figure 9: Estimated total Pb contents (a) and background (b) based on the whole dataset (581 data). The black circle shows the local highly "polarized" estimations explained by the presence of a sample with high Pb contents (discarded in the reduced dataset).

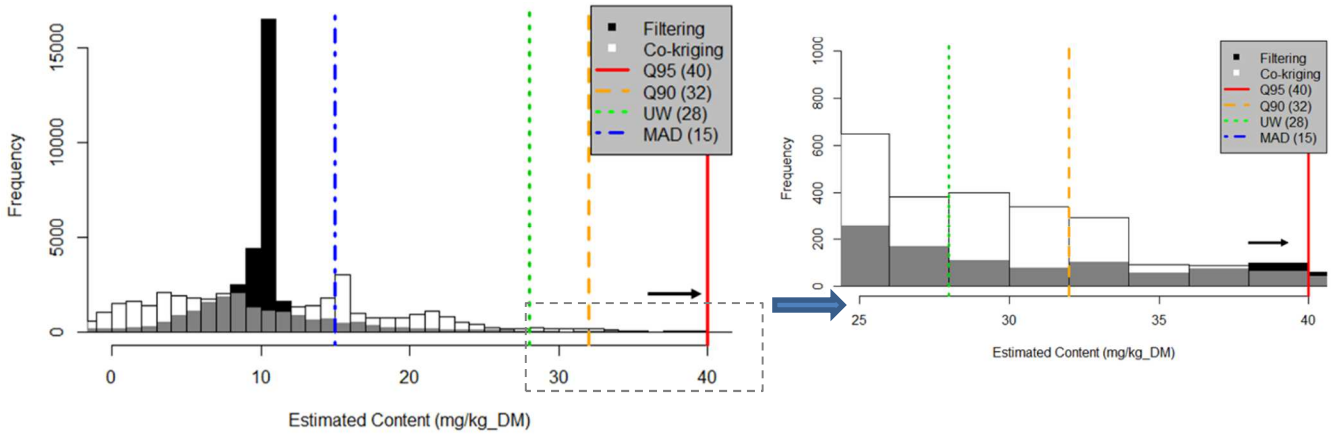

Figure 10: Histograms of estimated total Pb (grey and white) and background (grey and black) based on the multi-support dataset (581 data). The black arrow indicates graphic truncation (i.e. higher content not shown). Standard statistical thresholds values calculated on the whole dataset (581 data) are reported. MAD: median absolute deviation, UW: upper whisker, Q90: 90th percentile, Q95: 95th percentile. Units are mg/kg_DM.

4.3 Influence of the whole versus reduced datasets

Keeping only the data corresponding to similar sample lengths (reduced dataset) discards a significant portion of the data, which implies a significant loss of information (from 581 to 303 data). While the co-kriging maps based on the whole dataset (Figure 9) are relatively similar to those obtained with the reduced dataset (Figure 7), local differences appear nevertheless between the estimations, particularly at locations of point-source contamination. The histograms and correlation diagrams (Figure 11) confirm these differences. The histogram of the total Pb content estimations calculated with the whole dataset shows a higher proportion of extreme values, whereas the proportion of medium values is larger with the reduced dataset.

These differences can be explained by two phenomena. The first one is the influence of the discarded data in the reduced dataset. The second phenomenon is the influence of the vertical discretization of the sample support. When considering the whole dataset, each sample has its vertical variable extension and its gravity center is set at its “exact” vertical location (3D approach). In the 2D approach on the other hand, all samples are considered with the same lengths and at a common depth. The 3D approach distributes the data more faithfully along the vertical axis.

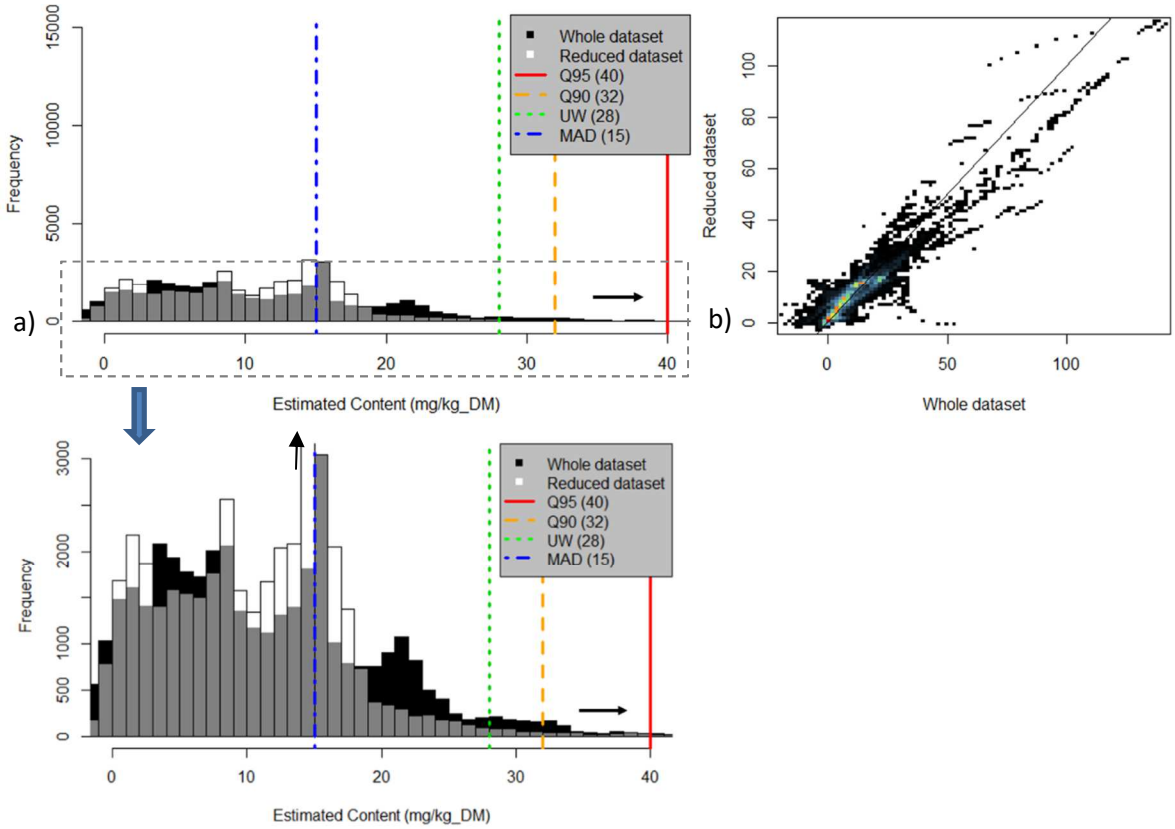

504

505
506 **Figure 11: a) Histogram of the total Pb contents estimations with the reduced dataset (white and grey) and the whole**
507 **dataset (black and grey). Bottom figure is a zoom. The black arrows indicate that higher values are not shown. Standard**
508 **statistical thresholds values calculated with the whole dataset (581 data) are reported. UW: upper whisker, Q90: 90th**
509 **percentile, Q95: 95th percentile. Units are mg/kg_DM. b) Correlation diagram between estimations obtained with whole**
510 **dataset (abscissa) and reduced dataset (ordinate).**

511 The differences are more significant on the background estimations (Figure 12). Some large
512 background estimations generated using the reduced dataset become low (and even negative) when
513 estimated from the whole dataset (Figure 11). As mentioned previously, the additional samples of
514 the whole dataset led to local strongly "polarized" estimations with high and low values (black circle
515 on Figure 9). On the correlation cloud (Figure 12b), the high estimates with the whole dataset are
516 thus associated to low estimates with the reduced dataset, which generates a local negative
517 correlation. In addition, the histogram (Figure 12a) clearly reflects the influence of discarding the low
518 values in the reduced dataset (Figure 4). Indeed, the mode is clearly lower for the whole dataset
519 (581 data), than for the reduced one (303 data). This is consistent with the observations from the
520 general statistics in Table 2. It emphasizes the influence of the data pre-processing (selection and
521 discretization).

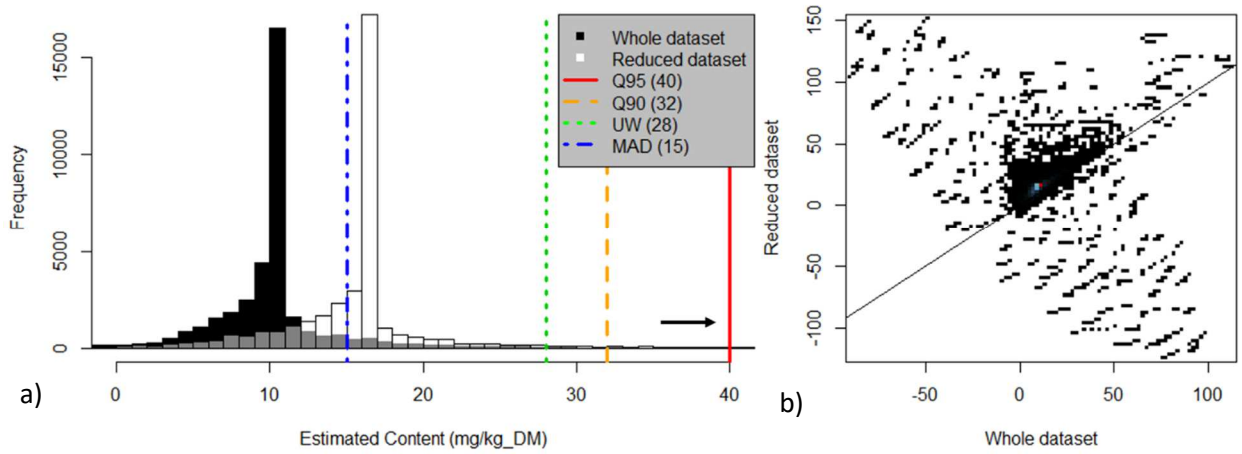

522
523
524 **Figure 12: a) Histogram of the Pb background estimated by filtering based on the reduced dataset (white and grey) or**
525 **on the whole dataset (black and grey). The black arrow indicates data truncation (i.e. highest values not shown).**
526 **Standard statistical thresholds values calculated on the whole dataset (581 data) are reported on the histogram. UW:**
527 **upper whisker, Q90: 90th percentile, Q95: 95th percentile. Units are mg/kg_DM. b) Scatter diagram between the**
528 **estimation with the whole dataset in abscissa and the reduced dataset in ordinate.**

529

530 Finally, the standard deviations of estimation error maps (Figure 13) are different for both
531 estimations (co-kriging vs. filtering) and depend on the dataset used. The blue spots (low standard
532 deviation) are more frequent in the background map based on the whole data set than in the case of
533 the reduced dataset. Figure 14 clearly shows that adding data decreases the standard deviation of
534 the estimation errors. The opposite effect may sometimes occur, due to the consideration of the
535 exact sample location in 3D.

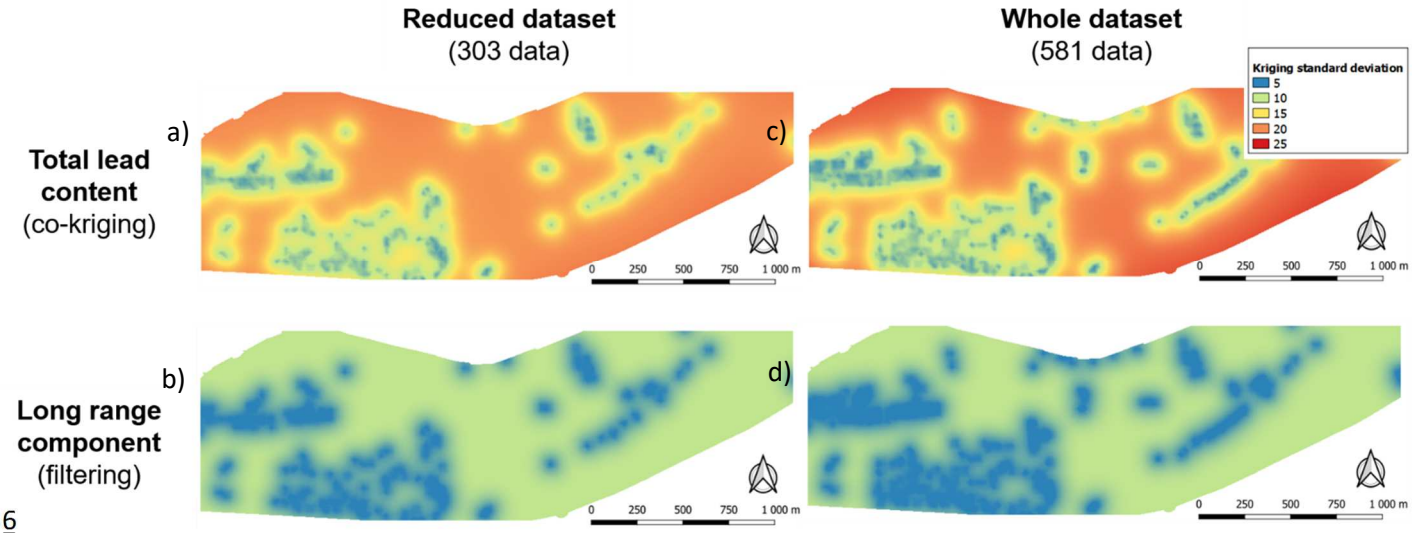

536
537 **Figure 13: Standard deviation of the estimation error maps for Pb total contents by co-kriging (a & c) and background**
538 **by filtering (b & d) based on the reduced dataset (a & b) and on the whole dataset (c & d).**

539

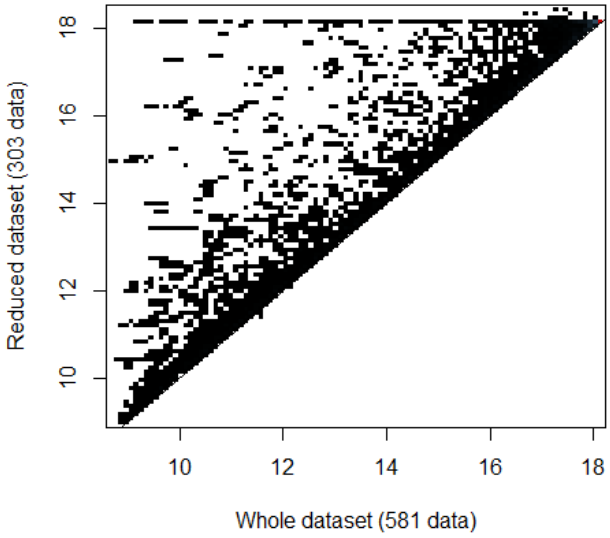

Figure 14: Correlation diagram of standard deviation of the background estimation according to the dataset (reduced dataset versus whole dataset).

4.4 Discussion

Since the data originate from pollution diagnostic studies, the whole dataset introduces biases related to the specific initial objectives of the data. This approach does not fulfill the recommendations issued by the group of geochemical experts (Demetriades and Birke, 2015) who advise a systematic strategy for mapping the urban pedo-geochemical (URGE) background. Another difference is due to the investigation depth. The sampling used to determine the pedo-geochemical background (whether urban or not) typically focuses on topsoils (Albanese, 2007; Demetriades and Birke, 2015; Karim *et al.*, 2015; Lark and Scheib, 2013; Reimann and al., 2012; Saby *et al.*, 2006). But, given the reuse guidelines for excavated soils (Coussy et al., 2020), the subsoil must be taken into account and therefore, all available subsoil samples have been used with depths up to 5m. Then Geostatistical filtering appears as a relevant solution when the sole use of samples dedicated to the determination of the pedo-geochemical background is not possible.

Based on the variability scale, the filtered anomalies present not only high values (contamination) but also low values(areas with abnormally low metal contents), as opposed to statistical thresholds, which are only intended to highlight the highest ”outliers”. Therefore, in the presence of estimated negative anomalies, the background estimation produces values locally greater than those of the total content estimation. This may correspond to deposits of materials with lower contents than those of the surrounding materials in place.

It should also be noted that the estimated contents are influenced by data means, which themselves reflect the influence of large values. This effect could lead to a bias in the estimations (total and background contents) especially when the data come from surveys aimes at polluted site characterization. In such cases, the sampling may be biased, with a lack of low contents.

Moreover, the variable sample length may cause practical problems since the content variability depends on the support. Selecting samples with similar support facilitates the variogram modeling if the data are numerous enough, but should be avoided for the estimation, because it reduces the number of data. There is no theoretical difficulty to introduce the support explicitly in the co-kriging or filtering equations, which allows the utilization of all available data. This represents a significant gain in precision, and the estimations become more faithful to reality.

Also, taking into account the vertical extension and location of the samples is a more accurate reflection of the data. This leads to a reduction of the estimation error's standard deviation , in particular for the background component (Figure 14). However, taking into account the support implies working on variographic models (adaptation of the range and the nugget effect) and requires conceptual choices (size of the reference support, size of the discretization step) based on geostatistical expertise. In addition, the integration of new data can have consequences on the estimations; either globally (lower estimated values of the background component, Figure 12) or more locally (zone of contrasted estimates, Figure 9). The integrated data require an in-depth study to validate their use. In all cases, a preliminary exploratory data study constitutes a key methodological step.

The choice was made herein to assume that anomalies could be either positive or negative, which is relevant in a context of excavated soil reuse: the total content may be lower than the local background value. This model is therefore different from a description of the contents as the sum of positive quantities. It corresponds to a background content to which the natural or anthropic "anomalies" are rather superimposed. This latter description makes it necessary to add information, such as the absence or presence of local anomalies, or the local ratio between the mean of each spatial component (background and anomalies).

5 Conclusions

It is possible to separate out background from "anomalies" based on the estimation of the long-range component by filtering, relying on an interpretation of the linear model of coregionalization. For this, the use of correlated covariates makes the estimation more representative of the long-distance variations of the variable of interest. This methodology may be applied at various scales, but this has an influence on the type of anomalies being filtered. A phenomenon seen as an anomaly at a large scale might be considered as the background at a smaller scale.

Geostatistical filtering can also be applied to the data themselves, in order to detect high or low "outliers". Nevertheless, geostatistical estimations require a large amount of data, which is generally incompatible with the sampling budgets dedicated to the estimation of pedo-geochemical backgrounds in urban areas. To remedy this problem of data paucity, the use of pre-existing data is required, even though it may have been collected with different objectives than that of defining a pedo-geochemical background. Different sampling protocols rely on different supports and therefore influence the variability, complicating the variographic study. Taking into account the size of the support in the estimation represents a viable alternative in order to avoid a loss of information such as is the case if only considering data with similar support.

Several parameters, such as the spatial distribution of the samples or inter-variable correlations, must be taken into account and need a preliminary exploratory data analysis. These parameters help building the variogram model and identifying the additional data ultimately needed.

In conclusion, filtering is a common practice in fields requiring a separation between point and diffuse phenomena. It appears especially useful for creating reference values or studying the general properties of soils and subsoils, assuming that the linear model of coregionalization is relevant. It provides the opportunity to mine existing data, collected in different contexts, thus reducing the burden associated with additional sampling campaigns and associated costs.

Acknowledgments

The authors thank ADEME (PhD thesis n°TEZ15-42 and SUPRA project, convention n°1772C0033) and the Région *Pays de la Loire* (POLLUSOLS project) for their financial support. They also thank Samoa for allowing them to use the data collected on their district for research purposes.

References

ADEME, 2018. Méthodologie de détermination des valeurs de fonds dans les sols : Echelle territoriale. Groupe de travail sur les valeurs de fonds. 112 p.

Albanese, S., De Vivo, B., Lima, A., Cicchella, D., 2007. Geochemical background and baseline values of toxic elements in stream sediments of Campania region (Italy). J. Geochem. Explor., 93(1), 21-34. https://doi.org/10.1016/j.gexplo.2006.07.006

Alloway, B. J., 1990. Soil processes and the behaviour of metals. Heavy metals in soils., 7-28.

Ander, E. L., Johnson, C. C., Cave, M. R., Palumbo-Roe, B., Nathanail, C. P., Lark, R. M., 2013. Methodology for the determination of normal background concentrations of contaminants in English soil. Sci. Total Environ., 454, 604-618. https://doi.org/10.1016/j.scitotenv.2013.03.005

Baize, D., 2008. Eléments traces dans les sols : ne plus parler de “Bruit de fond”, Environnement et Technique N°281, 5, 25-30.

Birke, M., Rauch, U., 2000. Urban geochemistry: investigations in the Berlin metropolitan area. Environ. Geochem. Health, 22(3), 233-248. https://doi.org/10.1023/A:1026554308673

Birke, M., & Rauch, U., 1997. Geochemical investigations in the Berlin metropolitan area. Z. Angew. Geol. 43(1), 58–65, Hannover.

Bourennane, H., Salvador-Blanes, S., Cornu, S., King, D., 2003. Scale of spatial dependence between chemical properties of topsoil and subsoil over a geologically contrasted area (Massif central, France). Geoderma, 112(3-4), 235-251. https://doi.org/10.1016/S0016-7061(02)00309-9

Cave, M. R., Johnson, C. C., Ander, E. L., Palumbo-Roe, B., 2012. Methodology for the determination of normal background contaminant concentrations in English soils. Nottingham, UK, British Geological Survey, 32p.

Chilès, J. P., Delfiner, P., 1999. Geostatistics: Modeling Spatial Uncertainty, A John Wiley & Sons. Inc., Publication, ISBN-13, 978-0.

Cicchella, D., De Vivo, B., Lima, A., Albanese, S., Fedele, L., 2008. Urban geochemical mapping in the Campania region (Italy). Geochem.: Explor., Environ., Analysis, 8(1), 19-29.https://doi.org/10.1144/1467-7873/07-147

Coussy, S., Hulot, C., Billard, A., 2017. Guide de valorisation hors site des terres excavées issues de sites et sols potentiellement pollués dans des projets d’aménagement. Ministère de la transition écologique et solidaire, 62p.

Daniau, C., Dor, F., Denys, S., Floch-Barneaud, A., Dab W., 2009. Problèmes posés par la définition de l'état de référence des sols en santé environnementale. In Annales des Mines-Responsabilité et environnement N°2, pp. 70-77. ESKA. https://doi.org/10.3917/re.054.0070

de Fouquet, C., 2011. From exploratory data analysis to geostatistical estimation: examples from the analysis of soil pollutants. Europ. J Soil Sci., 62(3), 454-466. https://doi.org/10.1111/j.1365-2389.2011.01374.x

de Fouquet, C., 2019. Exercices corrigés de géostatistique. Presses des mines**.** 320p.

Demetriades, A., Birke, M., 2015. Urban Topsoil Geochemical Mapping Manual (URGE II). EuroGeoSurveys, Brussels.

Edmondson, J.L., Davies, Z.G., McHugh, N., Gaston, K.J., Leake, J.R., 2012. Organic carbon hidden in urban ecosystems. Sci. Rep. 2. https://doi.org/10.1038/srep00963

672 Goovaerts, P., 1992. Factorial co-kriging analysis: a useful tool for exploring the structure of
673 multivariate spatial soil information. J. Soil Sci., 43(4), 597-619.
674 https://doi.org/10.1111/j.1365-2389.1992.tb00163.x
675 Hartley, W., Uffindell, L., Plumb, A., Rawlinson, H. A., Putwain, P., Dickinson, N. M., 2008. Assessing
676 biological indicators for remediated anthropogenic urban soils. Sci. Total Environ., 405(1-3),
677 358-369. https://doi.org/10.1016/j.scitotenv.2008.06.004
678 ISO 11074., 2005. Qualité du sol -Vocabulaire.
679 Jarva, J., Ottesen, R. T., Tarvainen, T., 2014. Geochemical studies on urban soil from two sampling
680 depths in Tampere Central Region, Finland. Environ. Earth Sci., 71(11), 4783-4799.
681 Karim, Z., Qureshi, B. A., Mumtaz, M., 2015. Geochemical baseline determination and pollution
682 assessment ofheavy metals in urban soils of Karachi, Pakistan. Ecolog. Indicators, 48, 358-
683 364. https://doi.org/10.1016/j.ecolind.2014.08.032
684 Lark, R.M., Scheib, C., 2013. Land use and lead content in the soils of London. Geoderma, 209, 65-74.
685 https://doi.org/10.1016/j.geoderma.2013.06.004
686 Le Guern, C., Sauvaget, B., with contributions from Campbell, S.D.G., Pfleiderer, S., 2017a. A review
687 of good practice and techniques in sub-urban geochemistry; to ensure optimal information
688 use in urban planning, COST TU1206 Working Group 2. Work package 2.6 report; TU1206-
689 WG2-008. (available from www.sub-urban.eu)
690 Le Guern, C., Baudouin, V., Bridier, E., Cottineau, C., Delayre, M., Desse-Engrand, F., Grellier, M.,
691 Milano, E., Mouny, A., Pollett, S., Sauvaget, B., Ménoury, A., Bâlon, P. with contribution from
692 Conil, P., Rouvreau, L., 2016a. Développement d'une méthodologie de gestion des terres
693 excavées issues de l'aménagement de l'Ile de Nantes - Phase 1 : Caractérisation des sols et
694 recensement des sources de pollution potentielles. Rapport BRGM/RP-66013-FR, 122 p., 27.
695 Ill., 7 Annexes. (https://infoterre.brgm.fr/rapports/RP-66013-FR.pdf)
696 Le Guern, C., Baudouin, V., Sauvaget, B., Delayre, M., Conil, P., 2016b. A typology of anthropogenic
697 deposits as a tool for modeling urban subsoil geochemistry: example of the Ile de Nantes
698 (France). J. Soils Sediments, 18(2), 373-379. https://doi.org/10.1007/s11368-016-1594-z
699 Le Guern, C., 2017b. Urban Geochemistry: from 2D to 3D, Procedia Engineering 209:26-33,
700 https://doi.org/10.1016/j.proeng.2017.11.126
701 Leys, C., Ley, C., Klein, O., Bernard, P., Licata, L., 2013. Detecting outliers: Do not use standard
702 deviation around the mean, use absolute deviation around the median. J. Exp. Social
703 Psychology, 49(4), 764-766. https://doi.org/10.1016/j.jesp.2013.03.013
704 Madrid, L., Diaz-Barrientos, E., Ruiz-Cortés, E., Reinoso, R., Biasioli, M., Davidson, C.M., Duarte,
705 A.C., Grcman, H., Hossack, I., Hursthouse, A., Kralj, T., Ljung, K., Otabbong, E., Rodrigues, S.,
706 Urquhart, G.J., Ajmone-Marsan, F. (2006) Potentially toxic metals in urban soils of six
707 European cities: a pilot study on selected parks. J. Environ. Monitor. 8, 1158–1165.
708 Matheron, G., 1965. Les variables régionalisées et leur estimation: une application de la théorie des
709 fonctions aléatoires aux sciences de la nature. Masson, Paris.
710 Matheron, G., 1982. Pour une analyse krigeante des données régionalisées. Centre de Géostatistique,
711 Rapport N-732, Fontainebleau, France.
712 McIlwaine, R., Cox, S. F., Doherty, R., Palmer, S., Ofterdinger, U., McKinley, J. M., 2014. Comparison
713 of methods used to calculate typical threshold values for potentially toxic elements in soil.
714 Environ. Geochem. Health, 36(5), 953-971. https://doi.org/10.1007/s10653-014-9611-x
715 Pouyat, R. V., Yesilonis, I. D., Russell-Anelli, J., & Neerchal, N. K., 2007. Soil chemical and physical
716 properties that differentiate urban land-use and cover types. Soil Sci. Society America
717 J., 71(3), 1010-1019. https://doi.org/10.2136/sssaj2006.0164
718 Raciti, S.M., Hutyra, L.R., Finzi, A.C., 2012. Depleted soil carbon and nitrogen pools beneath
719 impervious surfaces. Environ. Pollut. 164, 248–251.
720 https://doi.org/10.1016/j.envpol.2012.01.046
721 Reimann, C., Fabian, K., Birke, M., Filzmoser, P., Demetriades, A., Négrel, P., Anderson, M., 2018.
722 GEMAS: Establishing geochemical background and threshold for 53 chemical elements in
723 European agricultural soil. Appl. Geochem., 88, 302-318.

Reimann, C., de Caritat, P., 2017. Establishing geochemical background variation and threshold values for 59 elements in Australian surface soil. Sc. Total Environ., 578, 633-648. https://doi.org/10.1016/j.scitotenv.2016.11.010

Reimann, C., Flem, B., Fabian, K., Birke, M., Ladenberger, A., Négrel, P., Team, T. G. P., 2012. Lead and lead isotopes in agricultural soils of Europe–The continental perspective. Appl. Geochem., 27(3), 532-542. https://doi.org/10.1016/j.apgeochem.2011.12.012

Reimann, C., Filzmoser, P., Garrett, R. G., 2005. Background and threshold: critical comparison of methods of determination. Sci. Total Environ., 346(1), 1-16.

Rivoirard, J., 2003. Cours de géostatistique multivariable. Cours C-172, CG, Ecole des Mines de Paris, France.

Rodrigues, S., Urquhart, G., Hossack, I., Pereira, M. E., Duarte, A. C., Davidson, C., Roberston, D., 2009. The influence of anthropogenic and natural geochemical factors on urban soil quality variability: a comparison between Glasgow, UK and Aveiro, Portugal. Environ. Chem. Let., 7(2), 141-148. https://doi.org/10.1007/s10311-008-0149-y

Rothwell, K. A., Cooke, M. P., 2015. A comparison of methods used to calculate normal background concentrations of potentially toxic elements for urban soil. Sci. Total Environ., 532, 625-634. https://doi.org/10.1016/j.scitotenv.2015.06.083

Saby, N. P. A., Thioulouse, J., Jolivet, C. C., Ratié, C., Boulonne, L., Bispo, A., Arrouays, D., 2009. Multivariate analysis of the spatial patterns of 8 trace elements using the French soil monitoring network data. Sci. Total Environ., 407(21), 5644-5652. https://doi.org/10.1016/j.scitotenv.2009.07.002

Saby, N., Arrouays, D., Boulonne, L., Jolivet, C., Pochot, A., 2006. Geostatistical assessment of Pb in soil around Paris, France. Sci. Total Environ., 367(1), 212-221. https://doi.org/10.1016/j.scitotenv.2005.11.028

Sauvaget, B., 2019. Constitution de référentiel géochimique locaux pour les sols et proches sous-sols urbains : de la base de données à l'interprétation géostatistique (pHD Thesis, Mines ParisTech, Paris, France), 214p.

Sauvaget, B., de Fouquet, C., Le Guern, C., Brunet, J-F., Belbeze, S., Roussel, H., 2020. Anticipating geochemical compatibility to reuse excavated soils at urban scale: are statistical tools effective? J. Geochem. Explor., 213. https://doi.org/10.1016/j.gexplo.2020.106522

Tarvainen, T., Jarva, J., 2011. Using geochemical baselines in the assessment of soil contamination in Finland. In: Johnson C.C., Demetriades A., Locutura O., & Ottosen R. T. (eds), Mapping the Chemical Environment of Urban Areas, John Wiley, Oxford, pp. 223-231. https://doi.org/10.1002/9780470670071.ch15

Wackernagel, H., 2003. Multivariate Geostatistics, Third edition, Springer-Verlag, Berlin, 387 p.

Wackernagel, H., Sanguinetti, H., 1993. Gold prospection with factorial cokriging in the Limousin, France. In: Davis, J.C. and Herzfeld, U.C. (Ed.) Computers in Geology: 25 years of progress. Studies in Mathematical Geology, Vol. 5, 33–43, Oxford University Press, Oxford.